Ultrasensitive detection of RNA biomarkers using portable sensing platforms based on organic electrochemical transistors

Ying Fu,[1,2] Naixiang Wang,[1] Anneng Yang,[1] Zhiai Xu,[3] Wen Zhang,[3] Hong Liu,[1] Helen Ka-wai Law,[4] and Feng Yan[1, 5]*

[1]Department of Applied Physics, The Hong Kong Polytechnic University, Hung Hom, Kowloon, Hong Kong.

[2]Department of Pure and Applied Chemistry, Technology and Innovation Centre, University of Strathclyde, Glasgow G1 1RD, UK

[3]School of Chemistry and Molecular Engineering, East China Normal University, Shanghai 200062, P. R. China

[4]Department of Health Technology and Informatics, Faculty of Health and Social Sciences, The Hong Kong Polytechnic University, Hong Kong.

[5]Research Institute of Intelligent Wearable Systems, The Hong Kong Polytechnic University, Hung Hom, Kowloon, Hong Kong.

*e-mail: apafyan@polyu.edu.hk

ABSTRACT

The analysis of RNA plays an important role in the early diagnosis of diseases and will greatly benefit patients with a higher cure rate. However, the low abundance of RNA in physiological environments requires ultrahigh sensitivity of a detection technology. Here, we construct a portable and smart-phone-controlled biosensing platform based on disposable organic electrochemical transistors for ultrasensitive analysis of micro RNA (miRNA) biomarkers within 1 hour. Due to their inherent amplification function, the devices can detect miRNA cancer biomarkers from little-volume solutions with concentrations down to 10^{-14} M. The devices can distinguish blood miRNA expression levels at different cancer stages using 4T1 mouse tumor model. The technique for ultrasensitive and fast detection of RNA biomarkers with high selectivity opens a window for mobile diagnosis of various diseases with low cost.

Keywords: organic electrochemical transistors, biosensor, RNA, cancer biomarker

INTRODUCTION

The effective control of many life-threatening diseases like cancer relies upon early diagnosis.[1-3] Conventional detection techniques based on large facilities in hospitals or laboratories often need large sample volume, complex protocol and long testing time.[4] Convenient and cost effective techniques are urgently needed for such applications.[5] The analysis of biomarkers, like micro RNAs (miRNAs), has been widely used for the early diagnosis of cancer.[6, 7] MiRNAs are regulatory RNA molecules with a length of about 21~23 nucleotides,[8] whose expression is often dysregulated in cancer.[9-11] It appears to be ideal targets for cancer regular monitoring due to their quantifiable and stable status in a variety of body fluids including blood, saliva and urine.[12, 13] More importantly, blood miRNAs are highly specific and their expression profiles differ among the developmental stages of tumors, and thus can be regarded as essential biomarkers for early cancer monitoring.[14, 15] Furthermore, RNA analysis has been proven to be rapid and reliable testing technology for many other diseases, like Coronavirus disease 2019 (COVID-19).[16] The standard RNA profiling techniques are microarrays, electrophoresis and reverse transcription polymerase chain reaction (RT-PCR).[17] Microarrays and electrophoresis suffer the limitation of low sensitivity while RT-PCR has the disadvantages of high cost, slow process and labor consuming.[18] With the increasing demand for portable monitoring of RNA,[19] the development of convenient methods with high sensitivity and selectivity is necessary.

Nowadays, organic thin-film transistors (OTFTs) have emerged as a versatile sensing platform for cost-effective, easy-to-use, portable, and disposable biosensors.[20-22] Organic electrochemical transistor (OECT) is a type of OTFT with a simple structure.[21, 23] A thin layer of organic semiconductor is deposited on the channel area between the source and drain electrodes and exposed to electrolyte together with the gate electrode.[24, 25] Compared to other transistor-based sensors (e.g. 2D material-based transistors, organic FET, etc), OECT has the advantage of low cost and high stability in aqueous solutions.[26] OECTs have been extensively investigated for high-performance biosensing such as glucose,[27] dopamine[28] and cell.[29] However, nucleic acid biosensors

based on OECTs reported before are not sensitive enough to detect the trace amount of specific miRNA biomarkers (~ several pg/L) in real physiological environments.[30]

In this paper, we construct an ultrasensitive portable monitoring platform based on OECTs for the analysis of miRNAs expression levels at different cancer stages. MiR-21, one of the most important and well-studied miRNA biomarker that promotes cell growth and metastasis,[31-32] is chosen as the detection target. MiR-21 is captured on the gate electrode and then specifically recognized by a nanoprobe with catalytic electrochemical activity. The device can detect several μL of miR-21 solution (one drop solution) within 1 hour with a good selectivity and a low detection limit down to 10^{-14} M. The miR-21 expression levels in different kinds of cells are clearly differentiated. More importantly, the devices successfully demonstrate distinct miRNA expressions at different cancer stages in blood samples using 4T1 tumor model and identify an early cancer stage from normal and other cancer stages. By simply replacing the capture and probe DNA sequence, the sensor can be applied in the detection of many other miRNA biomarkers. Therefore, this approach provides a versatile tool to conveniently monitor various RNA biomarkers with low sample volume for the diagnosis of many diseases like cancer and COVID-19.

RESULTS

The design of device and portable monitor system

Figure 1A shows the architecture of the portable monitor system, which can be divided into three components including a flexible and transparent miRNA OECT sensor (Figure S1A), a meter with readout circuit and a smart phone with a user application program. The sensor is inserted into the meter, and the meter can be remotely controlled by the smart phone via Bluetooth. The transfer curve (I_{DS} vs. V_G) of the device and the channel current response (I_{DS} vs. time) upon different concentrations of the target miRNA can be recorded by the user application program in the smart phone (Figure S1B, C).

The OECT device is prepared on a flexible plastic substrate by photolithography for disposable applications. Figure 1B illustrates the device design of the OECT-based miRNA sensor, in which the patterned gold electrodes serve as source, drain, and gate of the device. Poly(3,4-ethylenedioxythiophene) polystyrene sulfonate (PEDOT:PSS) is spin coated and patterned in the channel region. The gate electrode is modified with capture DNA, miRNA, and probe DNA with enzyme horseradish peroxidase (HRP). Since HRP has high catalyze activity toward H_2O_2,[33] the channel current response of the OECT is characterized after adding H_2O_2 (100 μM) in its electrolyte.[34]

The gate modification progress is shown in Figure 1C. 3'-SH modified capture DNA is first anchored on the gate electrode via a strong SH-Au binding (CV and EIS characterization in Figure S2).[35] Target miRNA (PBS or purified solution from cells and blood) can be selectively captured on the gate electrode. Probe DNAs modified with nanoprobes are incubated on the electrode surface to form a typical sandwich format.[36] The nanoprobes are synthesized by using gold nanoparticles (Au NPs) as substrate to bind with biotin and HRP and characterized by UV-vis spectrum and transmission electron microscope (Figure S3). Au NPs have good conductivity and large surface area for binding electrochemical segments. Biotin on the nanoprobes can specially link to the streptavidin (SA) on the tail of the probe DNA with the binding rate of biotin to SA being 1 to 4.38.[37] Thus, a single target miRNA can attach probe DNA with several nanoprobes. Figure 1D exhibits the operation of an OECT in an electrolyte in the presence of the enzymatic reaction. There is no charge transfer at the gate electrode without H_2O_2. [38]

Upon the addition of H_2O_2, direct electron transfer occurs between the heme group (Fe(III)/Fe(II)) of HRP in the nanoprobe and the electrode surface.[39,40] Under a positive gate voltage (V_G) , the Faradic current due to the electrocatalytic reaction decreases the

potential drop at the gate/electrolyte interface, and subsequently increases the effective gate voltage (ΔV_G^{eff}) applied on the channel. [41-42] Figure 1E shows the potential distribution at the gate/electrolyte and electrolyte/channel interfaces under a gate voltage. The reaction of H_2O_2 at the gate will change the potential distribution as demonstrated by the dash line. The relationship between ΔV_G^{eff} and the amount of HRP (W_{HRP}) modified on the gate is listed in supporting information.[34]

MiRNA biomarker analysis and selectivity test

Figure 2A shows the channel current responses upon H_2O_2 addition of OECT with miRNA solutions with different concentrations. The change in the channel current (ΔI_{DS}) monotonically increases with the increase of miRNA concentration in a wide range between 10^{-15} and 10^{-6} M. According to the transfer curve (I_{DS} vs V_G) in Figure S3, ΔV_G^{eff} of the device is calculated and presented in Figure 2B, which shows a good liner relationship with the miRNA concentration on logarithmic axis. The detection limit (Signal to noise ratio >3) of the miRNA sensor is about 10^{-14} M. The ultrahigh sensitivity of the OECT-based sensor can be attributed to the signal amplification by the transistor.[43, 44]

Figure S5A shows miR-21 detection by cyclic voltammogram (CV) measurements with concentrations ranging from 10^{-6} M to 10^{-11} M, which indicates the successful gate modification. It is also confirmed by fluorescence images (See Figure S6). As shown in the selectivity testing in Figure S5B, the device modified with three-base mismatched miRNA demonstrates no response with concentration of 10^{-3} M. To show the versatility of the sensing platform, simply changing the sequences of capture DNA and probe DNA accordingly, another cancer biomarker (hsa-miR-16) is detected.[45] It shows a linear response to miRNA concentration ranging from 10^{-6} M to 10^{-14} M, exhibiting a similar detection limit of 10^{-14} M (Figure S7).

MiRNA biomarker analysis in cells

The OECT sensors are used to detect miRNA expression in cells, including MCF-7 (breast cancer cell, poorly metastatic), MDA-MB-231 (breast cancer cell, highly

metastatic) and NIH/3T3 (normal cell, from mouse fibroblast). All cell lines were cultured to extract miRNA using the same protocol (see supporting information). As shown in Figure 3A and Figure 3B, the calculated ΔV_G^{eff} from current change increase with the rising MDA-MB-231 cell concentrations from 10^1 cells/mL to 10^5 cells/mL. The insert of Figure 3b shows the fluorescence and optical images of MDA-MB-231 cells with a concentration of 10^5 cells/mL. The responses of the devices to MCF-7 cancer cells shown in Figure 3C and D are relatively lower. The lowest responses of the devices can be observed in the detection of NIH/3T3 normal cells as shown in Figure 3E and F. Since miR-21 is overexpressed in cancer cells than in normal cells, it is reasonable to find that miR-21 concentrations in MCF-7 and MDA-MB-231 are higher than that in NIH/3T3. For the two types of cancer cells, the invasion behavior of MCF-7 cells is relatively weak. MiR-21 is highly associated with cancer cell proliferation, migration and invasion, so its expression level is higher in MDA-MB-231 than MCF-7 cells.

Blood miRNA analysis in tumor mouse model

4T1 tumor model is developed by injecting 4T1 cancer cells into BALB/c mouse.[46] The 4T1 tumor has the advantages of easy transplant procedure and its progressive behavior is very similar to human mammary cancer.[47] The upregulation of miR-21 in blood is closely associated with 4T1 tumor progression, so it is assumed that miR-21 circulating in blood could show an increasing concentration with the growth of tumor.

Figure 4A shows images of BALB/c mouse in different cancer stages: normal, early, middle and late stages. The corresponding tumor sizes are: 0, 300, 600, 1000 mm^3. 100 μL of blood was taken from the mouse tumor model and underwent a standard purification progress to extract miRNAs (see supporting information). The obtained solution is miRNA mixture, which greatly challenges the sensitivity and selectivity of the detection method. As shown in Figure 4B, the responses of the devices treated with tumor blood samples are higher than those of the normal stage, and the amplitudes increase with the increase of tumor size. As shown in Figure 4C, ΔV_G^{eff} of the device

modified with a blood sample at the early stage tumor is higher than that of normal stage, which clearly indicates that the sensor can differentiate blood samples in early cancer stage.

DISCUSSION

We have developed an ultrasensitive miRNA analysis by using OECTs. The device could specifically detect different cancer miRNA biomarkers from a little volume of solution with a concentration down to 10^{-14} M, which shows a much higher sensitivity than conventional electrochemical measurement. This OECT-based miRNA sensor demonstrates linear responses to a wide range of miRNA concentrations from 10^{-6} M to 10^{-14} M, which is sensitive enough to detect the trace amount of miRNA levels in cancer cells. The devices are successfully used to do miRNA expression analysis in blood samples from mouse tumor model and differentiate the miRNA levels in blood samples even for early cancer stage. Compared to other electrical sensors relying on electrochemical workstation, this sensing platform can provide convenient and portable detections of various RNA biomarkers for diagnostic monitoring of a wide range of diseases.

Supporting Information.

Materials, experimental details for device, gate modification, CV measurements, selectivity testing and all the supporting figures are listed in the supporting information.

ACKNOWLEDGMENTS

We acknowledge the funding support from the Research Grants Council of the Hong Kong Special Administrative Region (Grant No. PolyU 152087/17E).

AUTHOR CONTRIBUTIONS

FY conceived the experiments. YF, and NW fabricated and characterized the devices.

AY and HL helped with portable system characterization. ZW and ZX assisted some experiments on mouse tumor building. HL contributed to the cell analysis. The manuscript was written by YF and FY and discussed, edited and approved by all of the authors.

DECLARATION OF INTERESTS

The authors declare no competing interests.

REFERENCES

1 Ilbawi, A., Varghese, C., Loring, B., Ginsburg, O., Corbex, M. Guide to Cancer Early Diagnosis. World Health Organization, **2017**, 1-38.

2 Pannala, R., Basu, A., Petersen, G. M., Chari, S. T. New-onset diabetes: a potential clue to the early diagnosis of pancreatic cancer. *Lancet Oncol.* **2009**, 10, 88-95.

3 Bedard, N., Pierce, M., El-Naggar, A., Anandasabapathy, S., Gillenwater, A., Richards-Kortum, R. Emerging roles for multimodal optical imaging in early cancer detection: a global challenge. *Technol Cancer Res. Treat*. **2010**, 9, 211-217.

4 PRECISION Study Grp Collaborators. MRI-targeted or standard biopsy for prostate-cancer diagnosis. *N. Engl. J. Med.* **2018**, 378, 1767-1777.

5 Jafari S H, Saadatpour Z, Salmaninejad A, et al. Breast cancer diagnosis: Imaging techniques and biochemical markers. *J. Cell Physiol.* **2018**, 233(7), 5200-5213.

6 Calin G A, Croce C M. MicroRNA signatures in human cancers. *Nat. Rev. Cancer* **2006**, 6, 857-866.

7 Abak, A., Amini, S., Sakhinia, E., Abhari, A. MicroRNA-221: biogenesis, function and signatures in human cancers. *Eur. Rev. Med. Pharmacol. Sci*. **2018**, 22, 3094-3117.

8 Duttagupta, R., Jiang, R., Gollub, J., Getts, R. C., Jones, K. W. Impact of cellular miRNAs on circulating miRNA biomarker signatures. *PloS one* **2011**, 6, e20769.

9 Pritchard C C, Kroh E, Wood B, et al. Blood cell origin of circulating microRNAs: a cautionary note for cancer biomarker studies. *Cancer Prev. Res.* **2012**, 5, 492-497.

10 Jeffrey, S. S. Cancer biomarker profiling with microRNAs. *Nat. Biotechnol*. **2008**, 26, 400-401.

11 Fredsøe J, Rasmussen A K I, Mouritzen P, et al. Profiling of circulating microRNAs in prostate cancer reveals diagnostic biomarker potential. *Diagnostics*, **2020**, 10, 188.

12 Brase J C, Johannes M, Schlomm T, et al. Circulating miRNAs are correlated with tumor progression in prostate cancer. *Int. J. Cancer*, **2011**, 128, 608-616.

13 Kosaka, N., Iguchi, H., Ochiya, T. Circulating microRNA in body fluid: a new potential biomarker for cancer diagnosis and prognosis. *Cancer Sci.* **2010**, 101, 2087-2092.

14 Bianchi F, Nicassio F, Marzi M, et al. A serum circulating miRNA diagnostic test to identify asymptomatic high-risk individuals with early stage lung cancer. *EMBO Mol. Med*. **2011**, 3, 495-503.

15 Veerla S, Lindgren D, Kvist A, et al. MiRNA expression in urothelial carcinomas: important roles of miR-10a, miR-222, miR-125b, miR-7 and miR-452 for tumor stage and metastasis, and frequent homozygous losses of miR-31. *Int. J. Cancer*, **2009**, 124, 2236-2242.

16 Srivastava R, Daulatabad S V, Srivastava M, et al. SARS-CoV-2 contributes to altering the post-transcriptional regulatory networks across human tissues by sponging RNA binding proteins and micro-RNAs. *BioRxiv*. **2020**, doi: 10.1101/2020.07.06.190348.

17 Lao K, Xu N L, Yeung V, et al. Multiplexing RT-PCR for the detection of multiple miRNA species in small samples. *Biophys. Res. Commun*. **2006**, 343, 85-89.

18 Baskerville, S., Bartel, D. P. Microarray profiling of microRNAs reveals frequent coexpression with neighboring miRNAs and host genes. *RNA*, **2005,** 11, 241-247.

19 Pardee K, Slomovic S, Nguyen P Q, et al. Portable, on-demand biomolecular manufacturing. *Cell*, **2016**, 167, 248-259.

20 Liao C, Zhang M, Yao M Y, et al. Flexible organic electronics in biology: materials and devices. *Adv. Mater*. **2015**, 27, 7493-7527.

21 Lin, P., Yan, F. Organic thin-film transistors for chemical and biological sensing. *Adv. Mater*. **2012**, 24, 34-51.

22 Wang, N., Yang, A., Fu, Y., Li, Y., Yan, F. Functionalized organic thin film transistors for biosensing. *Acc. Chem. Res*. **2019,** 52, 277-287.

23 Rivnay, J., Inal, S., Salleo, A., Owens, R. M., Berggren, M., Malliaras, G. G. Organic electrochemical transistors. *Nat. Rev. Mater*. **2018,** 3, 1-14.

24 Liao, C., Zhang, M., Niu, L., Zheng, Z., Yan, F. Organic electrochemical transistors with graphene-modified gate electrodes for highly sensitive and selective dopamine sensors. *J. Mater. Chem.* B, **2014,** 2, 191-200.

25 Chen L, Fu Y, Wang N, et al. Organic electrochemical transistors for the detection of cell surface glycans. *ACS Appl. Mater. Interfaces*. **2018,** 10, 18470-18477.

26 Strakosas, Xenofon, Manuelle Bongo, and Róisín M. Owens. The organic electrochemical transistor for biological applications. *J. Appl. Polym. Sci.* **2015**, 132, 15.

27 Liao, C., Zhang, M., Niu, L., Zheng, Z., Yan, F. Highly selective and sensitive glucose sensors based on organic electrochemical transistors with graphene-modified gate electrodes. *J. Mater. Chem. B*, **2013,** 1, 3820-3829.

28 Tang, H., Lin, P., Chan, H. L., Yan, F. Highly sensitive dopamine biosensors based on organic electrochemical transistors. *Biosens. Bioelectron*. **2011,** 26, 4559-4563.

29 Lin, P., Yan, F., Yu, J., Chan, H. L., Yang, M. The application of organic electrochemical transistors in cell-based biosensors. *Adv. Mater*. **2010,** 22, 3655-3660.

30 Lin, P., Luo, X., Hsing, I. M., Yan, F. Organic electrochemical transistors integrated in flexible microfluidic systems and used for label-free DNA sensing. *Adv. Mater*. **2011,** 23, 4035-4040.

31 Zhao, W., Zhao, J. J., Zhang, L., Xu, Q. F., Zhao, Y. M., Shi, X. Y., Xu, A. G. Serum miR-21 level: a potential diagnostic and prognostic biomarker for non-small cell lung cancer. *Int. J. Clin. Exp. Med.* **2015,** 8, 14759.

32 Bica-Pop, C., Cojocneanu-Petric, R., Magdo, L., Raduly, L., Gulei, D., Berindan-Neagoe, I. Overview upon miR-21 in lung cancer: focus on NSCLC. *Cell Mol. Life. Sci*. **2018,** 75, 3539-3551.

33 Fu Y, Liu K, Sun Q, et al. A highly sensitive immunosensor for calmodulin assay based on enhanced biocatalyzed precipitation adopting a dual-layered enzyme strategy. *Biosens. Bioelectron*. **2014**, 56, 258-263.

34 Fu, Y., Wang, N., Yang, A., Law, H. K. W., Li, L., Yan, F. Highly sensitive detection of protein biomarkers with organic electrochemical transistors. *Adv. Mater*. **2017,** 29, 1703787.

35 Patel, Manoj K., et al. Electrochemical DNA sensor for Neisseria meningitidis detection. *Biosens. Bioelectron.* **2010**, 25, 2586-2591.

36 Chandrasekaran, A. R., Punnoose, J. A., Zhou, L., Dey, P., Dey, B. K., Halvorsen, K. DNA nanotechnology approaches for microRNA detection and diagnosis. *Nucleic. Acids. Res*. **2019,** 47, 10489-10505.

37 Chen, Y. H., Chien, W. C., Lee, D. C., Tan, K. T. Signal Amplification and Detection of Small Molecules via the Activation of Streptavidin and Biotin Recognition. *Anal. Chem*. **2019,** 91, 12461-12467.

38 Bernards, D. A., Macaya, D. J., Nikolou, M., DeFranco, J. A., Takamatsu, S., Malliaras, G. G. Enzymatic sensing with organic electrochemical transistors. *J. Mater. Chem*. **2008,** 18, 116-120.

39 Zhang D, Zhao H, Fan Z, et al. A highly sensitive and selective hydrogen peroxide biosensor based on gold nanoparticles and three-dimensional porous carbonized chicken eggshell membrane. *PloS one*, **2015,** 10, e0130156.

40 Mercante, L. A., Facure, M. H., Sanfelice, R. C., Migliorini, F. L., Mattoso, L. H., Correa, D. S. One-pot preparation of PEDOT: PSS-reduced graphene decorated with Au nanoparticles for enzymatic electrochemical sensing of H_2O_2. *Appl. Surf. Sci*. **2017,** 407, 162-170.

41 Cicoira, F., Sessolo, M., Yaghmazadeh, O., DeFranco, J. A., Yang, S. Y., Malliaras, G. G. Influence of device geometry on sensor characteristics of planar organic electrochemical transistors. *Adv. Mater.* **2010**, 22, 1012-1016.

42 Friedlein, J. T., McLeod, R. R., Rivnay, J. Device physics of organic electrochemical transistors. *Org. Electron*. **2018,** 63, 398-414.

43 Yang, A., Li, Y., Yang, C., Fu, Y., Wang, N., Li, L., Yan, F. Fabric organic electrochemical transistors for biosensors. *Adv. Mater*. **2018,** 30, 1800051.

44 Liu, S., Fu, Y., Xiong, C., Liu, Z., Zheng, L., Yan, F. Detection of bisphenol a using DNA-functionalized graphene field effect transistors integrated in microfluidic systems. *ACS Appl. Mater. Interfaces*, **2018,** 10, 23522-23528.

45 Zhang J, Song Y, Zhang C, et al. Circulating MiR-16-5p and MiR-19b-3p as two novel potential biomarkers to indicate progression of gastric cancer. *Theranostics*, **2015,** 5(7), 733.

46 Pulaski, B. A., & Ostrand-Rosenberg, S. Mouse 4T1 breast tumor model. *Curr. Protoc. Immunol*. **2000,** 39, 20-2.

47 Malekian, S., Rahmati, M., Sari, S., Kazemimanesh, M., Kheirbakhsh, R., Muhammadnejad, A., Amanpour, S. Expression of Diverse Angiogenesis Factor in Different Stages of the 4T1 Tumor as a Mouse Model of Triple-Negative Breast Cancer. *Adv. Pharm. Bull*. **2020,** 10, 323.

Figures:

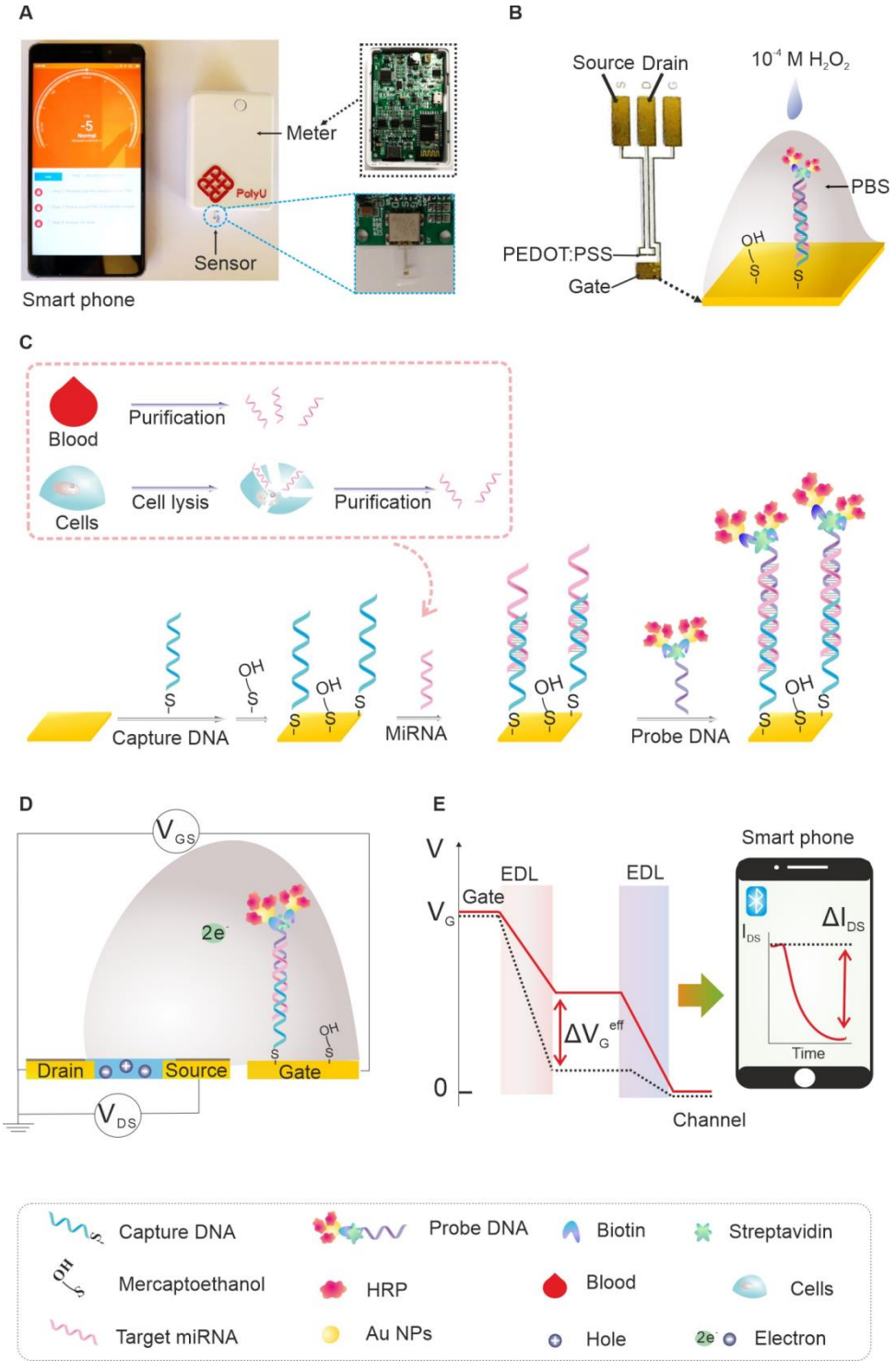

Figure 1. Design of OECT-based miRNA sensing platform.

(A) Scheme of the portable monitoring system with OECT based miRNA sensor. OECT miRNA sensor is inserted into a portable meter, and a smart phone is communicated with the portable meter via Bluetooth.

(B) Photo of an OECT miRNA sensor with three electrodes: drain, source and gate. An electrochemical reaction occurs on the gate electrode upon the addition of H_2O_2.

(C) The gate modification process for the detection of miRNA.

(D) An OECT with a functionalized gate characterized in a liquid electrolyte.

(E) The potential distribution in an OECT: potential drops between the gate and channel of the OECT before (dash line) and after (solid line) the addition of H_2O_2 in PBS solution. EDL is electrical double layer. The enzymatic reaction leads to ΔV_G^{eff} change and the corresponding I_{DS} change.

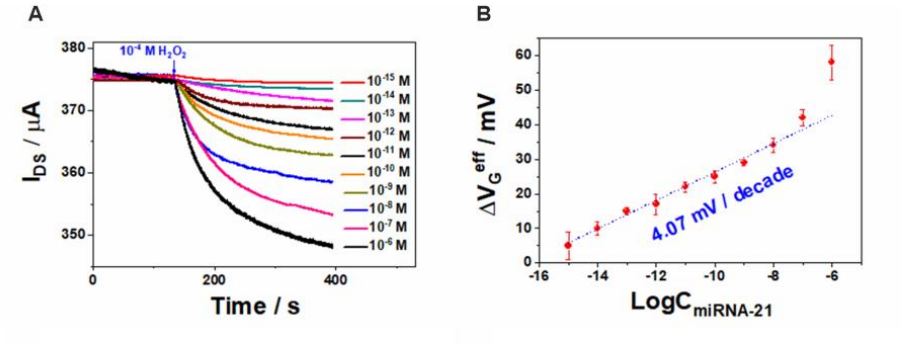

Figure 2. The response of sensors to miRNA (MiR-21) with different concentrations.

(A) OECT-based biosensors with nanoprobe-functionalized gate electrodes for the detection of a wide range miRNA concentration from 10^{-6} M to 10^{-15} M. The added H_2O_2 level was fixed at 100 μM for each addition (V_G= 0.7 V and V_{DS} = 0.05 V).

(B)Calculated ΔV_G^{eff} changes of the miRNA sensor as a function of miRNA concentration. The error bars were calculated from three parallel experiments.

(C)Standard three-electrode electrochemical detection of miRNA in the range of 10^{-6} M to 10^{-12} M by C-V measurements. The H_2O_2 level is 500 μM.

(D) The selectivity test of miRNA sensors by measuring three-base mismatched miRNA.

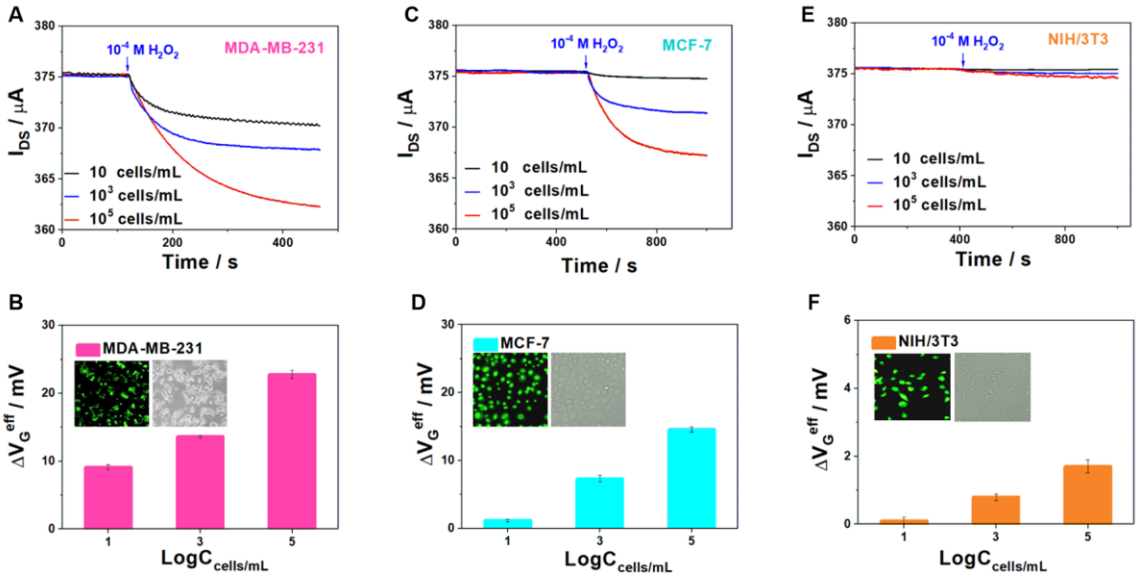

Figure 3. The responses of OECT-based miRNA sensors to the lysates of different cells.

(A) Current responses of OECTs in the detections of extracted miRNA solutions from different concentrations of MDA-MB-231 cancer cells: 10 cells/mL (black), 10^3 cells/mL (blue) and 10^5 cells/mL (red).

(B)Calculated ΔV_G^{eff} of OECTs in the detection of extracted miRNA solutions from MDA-MB-231 cancer cells with different concentrations. Inset: fluorescence (left) and optical images (right) of MDA-MB-231 cell with a concentration of 105 cells/mL.

(C)Current responses of OECTs in the detection of extracted miRNA solutions from different concentrations of MCF-7 cancer cells: 10 cells/mL (black), 10^3 cells/mL (blue) and 10^5 cells/mL (red).

(D) The calculated ΔV_G^{eff} corresponding to the responses. Insert: fluorescence (left) and optical images (right) of MCF-7 cell with a concentration of 10^5 cells/mL.

(E)Current responses of OECTs in the detection of NIH/3T3 normal cells and f. the calculated ΔV_G^{eff}. Insert: fluorescence (left) and optical images (right) of NIH/3T3 cell with a concentration of 10^3 cells/mL. All the error bars are calculated from at least 3 devices.

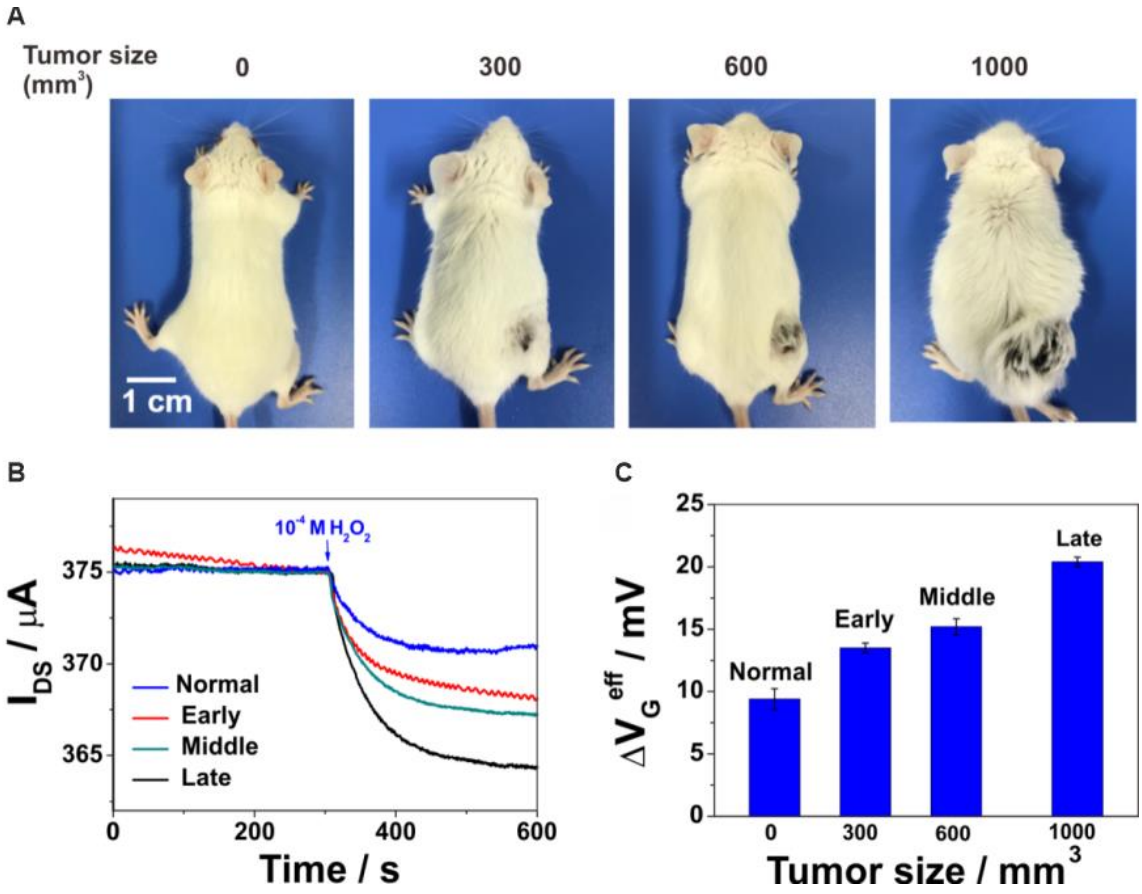

374

375 **Figure 4. The responses of miRNA sensors to the bloods from a mouse model with**
376 **different tumor sizes**

377 (A) Images of BALB/c mouse in different cancer stage: normal, early, middle and late. The
378 corresponding tumor sizes are: 0, 300, 600, 1000 mm^3.

379 (B) Current responses of the OECT sensors modified with blood miRNA samples at
380 different cancer stages and,

381 (C) The calculated ΔV_G^{eff} corresponding to the current change. The error bars are
382 calculated from three parallel experiments.

383

384 **For Table of Contents Only**

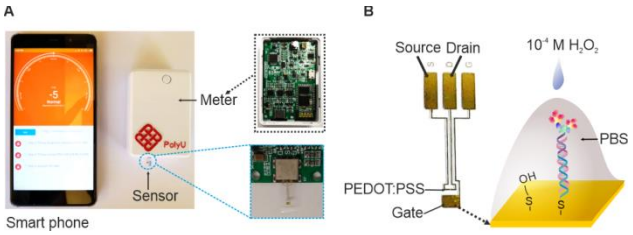

385